



# Engineered versus hybrid cellular vesicles as efficient drug delivery systems: a comparative study with brain targeted vesicles

Maria Kannavou<sup>1,2</sup> · Antonia Marazioti<sup>1,2</sup> · Georgios T. Stathopoulos<sup>3,4</sup> · Sophia G. Antimisiaris<sup>1,2</sup>

Accepted: 6 January 2021 / Published online: 20 January 2021  
© Controlled Release Society 2021

## Abstract

Herein we elaborated on methods to load cellular vesicles (CVs) and to incorporate cholesterol (Chol) and PEG lipids in their membrane, for enhancing the potential of such engineered CVs (e-CVs) as drug carriers. Hybrids formed by fusion between PEGylated liposomes (PEG-LIP) and CVs were evaluated as alternatives to e-CV, for the first time. Freeze-thawing cycles (FT) and incubation protocols were tested, and vesicle fusion was monitored by FRET dilution. B16F10, hCMEC/D3, and LLC cells were used for e-CV or hybrid development, and FITC-dextran as a model hydrophilic drug. Results show that dehydration rehydration vesicle (DRV) method is optimal for highest CV loading and integrity, while optimal protocols for Chol/PEG enrichment were identified. FT was found to be more efficient than incubation for hybrid formation. Interestingly, despite their high Chol content, CVs had very low integrity that was not increased by enrichment with Chol, but only after PEG coating; e-CVs demonstrated higher integrity than hybrids. Vesicle uptake by hCMEC cells is in the order: LIP < e-CVs < Hybrids ≤ CVs (verified by confocal microscopy); the higher PEG content of e-CVs is possibly the reason for their reduced cell uptake. While CV and hybrid uptake are highly caveolin-dependent, e-CVs mostly follow clathrin-dependent pathways. In vivo and ex vivo results show that brain accumulation of hybrids is only slightly higher than of CVs, indicating that the surface PEG content of hybrids is not sufficient to prevent uptake by macrophages of the reticuloendothelial system. Taking together with the fact that subjection of CVs to FT cycles reduced their cellular uptake, it is concluded that PEGylated e-CVs are better than hybrids as brain-targeted drug carriers.

**Keywords** Drug delivery · Exosomes · Mimetics · Cellular vesicles · Hybrid · Liposome · Uptake · FRET · In vivo · Biodistribution · Engineering

Maria Kannavou and Antonia Marazioti contributed equally to this work.

✉ Sophia G. Antimisiaris  
santimis@upatras.gr

<sup>1</sup> Laboratory of Pharmaceutical Technology, Department of Pharmacy, University of Patras, 26510 Rio, Greece

<sup>2</sup> Foundation for Research and Technology Hellas, Institute of Chemical Engineering Sciences, FORTH/ICE-HT, 26504 Rio, Greece

<sup>3</sup> Laboratory for Molecular Respiratory Carcinogenesis, Department of Physiology, Faculty of Medicine, University of Patras, 26510 Rio, Greece

<sup>4</sup> Comprehensive Pneumology Center (CPC), Institute for Lung Biology and Disease (iLBD), Helmholtz Center Munich–German Research Center for Environmental Health, Member of the German Center for Lung Research, 81377 Munich, Bavaria, Germany

## Abbreviations

B16	C57BL/6 mouse B16F10 skin melanoma cells
Chol	Cholesterol
CVs	Cellular vesicles
DiR	1,1-Dioctadecyl-3,3,3,3-tetramethylindotri-carbocyanine iodide
DLS	Dynamic light scattering
DRV	Dried reconstituted vesicles
FI	Fluorescence intensity
FITC	Fluorescein-isothiocyanate-dextran-4000
FVB	Friend leukemia virus B
hCMEC/D3	Immortalized human cerebral microvascular endothelial cells
LIP	Liposomes
LY	Lucifer yellow-CH dilithium salt
PC	1,2-Distearoyl-sn-glycerol-3-phosphatidyl-choline; hPC is hydrogenated-PC

PEG	1,2-Distearoyl-sn-glycerol-3-phosphoethanolamine-N-[methoxy(polyethyleneglycol)-2000]
PG	1,2-Distearoyl-sn-glycero-3-phospho-(1'-rac-glycerol) (sodium salt)
RHO	Lissamine rhodamine B phosphatidylethanolamine
NBD	1,2-Distearoyl-sn-glycero-3-phosphoethanolamine-N-(7-nitro-2-1,3-benzoxadiazol-4-yl) (ammonium salt)

## Introduction

It is generally accepted that extracellular vesicles (EVs) have opened exciting new horizons not only in therapeutics but also in drug delivery. The high organotropism of specific EV types initiated the founding of a new field in drug delivery, involving the design and development of novel EVs as targeted drug carriers [1–3]. In order to overcome the problems of low yield and multistep isolation of EV-derived vesicles, the use of whole cells was proposed as an alternative [4]. Cell-derived vesicles (CVs) represent a novel class of bioinspired drug delivery systems which, in contrary to exosomes, have high production yield, but similar protein and lipid composition with parental cells and EVs [5, 6]. Indeed, recent studies proved the applicability of CVs as drug carriers; in one case, doxorubicin-loaded CVs showed similar antitumor activity (in vivo), compared with doxorubicin-loaded EVs [4], while several other cases of successfully using CVs instead of EVs have been reported [7–12]. Such whole-cell-derived vesicles are referred as “top-down EV mimetics” [13, 14] to differ from “bottom-up EV mimetics” (or synthetic or chimeric EVs) [15] which are totally synthetic. CVs prepared from hepatocytes were recently found to efficiently promote liver regeneration after iv administration [12], while very good results were also obtained with plasmid-encapsulating engineered-CVs (e-CVs) designed as a gene-activated matrix that could locally release vascular endothelial growth factor (VEGF) for osteogenesis [16, 17].

Nevertheless, rapid accumulation of iv-injected CVs in the liver has been documented as a potential drawback for their applicability as drug carriers [11, 18]; similar problems have been also observed for EV drug carriers [19, 20]. As done for liposomes, modification of the surface of EVs with polyethylene-glycol (PEG) molecules (and in some cases also with targeting ligands), has been proposed as a method to prolong their circulation in blood and enhance their potential to target specific tissues [21].

In general, two methodologies can be applied for the modification of the surface of vesicles; one is to incubate the vesicles with PEG-lipid (or ligand-PEG-lipid) micelles,

and the other to prepare hybrid vesicles by fusion of the vesicles with liposomes (that have appropriate amounts of PEG-lipid or ligand-PEG-lipid in their lipid membrane). However, although both of the previous methodologies have been evaluated for development of improved EV drug carriers, they have not been considered for CVs. The only case of CV surface modification with PEG (PEGylation) was recently reported by our group [22], and involved the development of CVs derived from human brain endothelial cells (hCMEC/D3 cells) as brain-targeted drug carriers. In fact, enhanced brain accumulation of the PEGylated-CVs compared to the non-PEGylated ones was observed, and attributed to the potential prolongation of the CV blood circulation time due to PEGylation. The only other cases of CV modification reported involved the enrichment of red blood cell and platelet-derived vesicle membranes with cholesterol, as an approach to improve the retention of their therapeutic loads [23, 24].

To follow up on our recent results with brain-targeted CVs [22], we attempted herein to develop for the first time CV-liposome hybrid vesicles, and evaluate their potential as targeted drug carriers. Additionally, we further optimized CV engineering methodologies (for CV PEGylation and enrichment of CV membranes with cholesterol), and finally compared the hybrid (CV/liposome) vesicles with the optimized engineered CVs (e-CVs) for their potential as brain-targeted drug carriers.

## Materials and methods

1,2-Distearoyl-sn-glycerol-3-phosphatidylcholine (PC), 1,2-distearoyl-sn-glycero-3-phospho-(19-rac-glycerol) (sodium salt) (PG), 1,2-distearoyl-sn-glycerol-3-phosphoethanolamine-N-[methoxy (polyethyleneglycol)-2000] (PEG), 1,2-distearoyl-sn-glycero-3-phosphoethanolamine-N-(7-nitro-2-1,3-benzoxadiazol-4-yl) (ammonium salt) (NBD), and lissamine rhodamine B phosphatidylethanolamine (RHO) were purchased from Avanti Polar Lipids (Alabaster, AL). Cholesterol (99%) (Chol), Triton X-100 and fluorescein-isothiocyanate-dextran-4000 (FITC) were obtained from Sigma-Aldrich (Darmstadt, Germany). Lipophilic tracer, 1,1-dioctadecyl-3,3,3,3-tetramethylindotricarbocyanine iodide (DiR), which was used as the lipid-label in CVs for live animal imaging, was from Molecular Probes (Eugene, OR). Protein concentrations were measured by Bradford Micro Assay (Bio-Rad Laboratories, Hercules, CA). Chol concentration in samples was measured by an enzymatic method, using a kit from Biotechnological applications LTD (Athens, Greece). All blocking agents and inhibitors including chlorpromazine and filipin were purchased from Sigma-Aldrich (Darmstadt, Germany). All other chemicals were of analytical quality and were purchased from Sigma-Aldrich or Merck (Darmstadt, Germany).

The fluorescence intensity (FI) of samples was measured with a Shimadzu RF-1501 spectrofluorometer (Shimadzu, Kyoto, Japan) using EX-540/EM-590 nm for RHO detection and EX-490 nm/EM-525 nm for FITC or NBD detection; in all cases, 5-nm slits were used. A bath sonicator (Branson; Thermo Fisher Scientific, Waltham, MA) and microtip-probe sonicator (Sonics and Materials, Harborough, UK) were used for liposome and for CV preparation.

### Preparation of liposomes

Liposomes (LIP) composed of PC/Chol (2:1 mol/mol), PC/Chol/PEG (2.00:1.00:0.25 mol/mol), PC/PG/Chol (1.80:0.20:1.00 mol/mol), and PC/PG/Chol/PEG (9/1/5/1.3 mol/mol) (PEG-LIP) were prepared by the thin-film hydration method [25]. The thin lipid film was hydrated with PBS, pH 7.40. After initial formation of the liposome dispersions, their size was reduced by probe sonication (Sonics & Materials). Fluorescently labeled lipids (NBD-DMPE and RHO) were also prepared: PC/Chol (2/1) with 1 mol% NBD and 1 mol% RHO and PC/Chol/PEG (2/1/0.25) with 1 mol% NBD and 1 mol% RHO as above.

### Cell culture and CV formation

In the present study, human brain microvascular endothelial cells (hCMEC/D3), as well as mouse melanoma cells (B16F10 or B16), and mouse Lewis lung adenocarcinoma cells (LLCs) were used. The two latter cell types were used in order to test if the results of the applied CV engineering methodologies are specific for CVs derived from hCMEC/D3 cells, or if they can also be applied to CVs originating from other cells. B16F10 (B16) and LLC cells were grown in RPMI 1640 medium supplemented with 10% FBS and 1% antibiotic–antimycotic solution (Invitrogen, Carlsbad, CA, USA). The cells were cultured at 37 °C, 5% CO<sub>2</sub>/saturated humidity. Medium was changed every 2–3 days.

hCMEC/D3 cells [passage 25–35] were obtained under license from Institut National de la Sante et de la Recherche Medicale, INSERM, Paris, France, and were grown in RPMI 1640 medium supplemented with 10% FBS and 1% antibiotic–antimycotic solution (Invitrogen, Carlsbad, CA). In some cases, hCMEC/D3 cells were grown in EndoGro medium (Merck, Darmstadt, DE) supplemented with 10 mM HEPES, 1 ng/mL basic FGF (bFGF), 1.4 μM hydrocortisone, 5 μg/mL ascorbic acid, penicillin–streptomycin, chemically defined lipid concentrate, and 5% ultralow IgG FBS. All cultureware were coated with 0.1 mg/mL rat tail collagen type I (BD Biosciences, Franklin Lakes, NJ, USA).

CVs were derived from hCMEC/D3 cells, LLC, and B16 cells as described before [22]. Briefly, cells were incubated in T175 flasks until confluency, detached from the flasks with trypsin, and immediately washed 3 times with ice-cold PBS

and finally re-suspended in distilled water. Dispersions were probe sonicated (Sonics & Materials), for up to 3 min, and the CVs were isolated by ultracentrifugation (ThermoSorvall WX90 Ultra; Thermo Scientific) at 60,000 rpm for 2 h at 4 °C and re-suspended in PBS, pH 7.40.

### CV engineering methods

For drug loading, three methods, i.e., sonication, incubation, and dehydration/rehydration vesicle (DRV) method [26], were used following the same conditions described in detail before [22]. The only difference was that FITC (36 mM) was used as a model drug instead of calcein, in order to verify the previous results using a different substance as encapsulated drug model.

In all cases, vesicle phospholipid content was quantified by a method routinely used to measure the phospholipid content of liposomes [27]. The protein content of all cell-derived vesicles was quantified by the Bradford assay. CVs and liposome dispersions were extruded through polycarbonate membranes with pore sizes of 400 nm and 200 nm, in order to obtain nanosized vesicles.

In some cases, CVs were engineered (e-CVs) for enrichment of their lipid membrane with Chol and/or coating of their surface with PEG-lipids. Different conditions were tested, for optimization of the methodologies as explained in detail below.

### Addition of Chol in CV membranes

For Chol enrichment of the lipid membrane of CVs, two methods were evaluated: (i) incubation of CVs with a Chol/cyclodextrin complex (Chol-CD) (M1) and (ii) incubation of CVs with free Chol (dissolved in the liposome dispersion media) at 37 °C (M2).

In M1, a saturated hydroxyl-propyl-beta cyclodextrin (HPβCD)-Chol complex was prepared and used (as an efficient cholesterol donor) [28]. For the preparation of the complex, Chol was added in excess to an HPβCD solution (100 mg/mL) and the mixture was magnetically stirred for 5 days. Then, the samples were centrifuged and the supernatant was filtered, in order to remove any insoluble amount of Chol; the fraction of Chol which is complexed by the cyclodextrin (Chol-CD complex) forms a clear solution [29]. CVs (from B16 and hCMEC/D3 cells) in PBS (1 mg/mL phospholipid) were then incubated with the Chol-CD complex at 1/5 (v/v) ratio, under shaking, at 25 °C or 37 °C, for pre-determined time periods and after that samples were centrifuged and precipitated, CVs were washed twice to remove any excess of inclusion complex, and finally re-suspended in PBS.

For M2, CVs (dispersed in H<sub>2</sub>O) were incubated with Chol at 10%, 50% or 100% (w/w) at 37 °C. After

incubation, H<sub>2</sub>O was exchanged with PBS [23, 24]. For both methods, M1 and M2, 30-min and 2-h incubation periods were tested. The incorporation of Chol in CVs was measured after purification of the samples from free Chol (by size exclusion chromatography), by the CO/PAP enzymatic method [30, 31]. For this, 50 µl of each CV sample (after dilution with equal volume of ethanol in order to dissolve the CVs) were mixed with 1 mL of the reagent solution provided with the kit. After vigorous vortex agitation the samples were incubated for 15 min at 37 °C. The Chol content was calculated by the sample OD-510 nm, according to a calibration curve constructed from standard solutions of Chol in ethanol (50–1000 ppm). Initially, hPC/Chol liposomes with varying concentrations of Chol were constructed and measured, for verification of the accuracy of the method.

### PEGylation of CVs

For PEGylation, CVs (from B16 cells, which were used in this study due to their fast proliferation, compared with hCMEC/D3 cells) were initially PEGylated by incubation with different amounts of PEG micelles, for 2 h at 60 °C and then overnight at 4 °C, as previously reported [21]. PEG was used at 9 mol%, 10 mol%, and 12 mol% concentrations (compared to the total lipid content of CVs). Since CVs have negative zeta potential values, when PEG lipid is successfully incorporated in their membranes, their zeta potential value decreases; thereby, zeta potential decrease can be used as a measure of the degree of PEGylation. Finally, the best PEG concentration (the one resulting in the lowest zeta potential) was used in the next step of

optimization of the PEGylation methodology. Three CV/PEG-micelle incubation conditions were evaluated: 37 °C for 3 h, 60 °C for 1 h, and 60 °C for 2 h. Finally, PEG-CVs from hCMEC/D3 cells were prepared by the optimized method identified from the results of this set of experiments and were used in all the following studies.

### Formation of hybrids by fusion of liposomes and CVs (hybrid-CVs)

Initially, the fusion of liposomes was tested, using different formulations of liposomes, in order to adjust the experimental conditions for optimal formation of hybrids by fusion between liposomes and CVs. In a first study (S1), fusion between non-charged liposomes was evaluated, using PC/Chol liposomes (with no fluorescent labels) and similar liposomes that were labelled with 1 mol% NBD and 1 mol% RHO. The two types of liposomes (labelled and non-labelled) were then mixed (1:1 by volume), and the mixtures were sonicated and incubated or freeze-thawed using different time periods and temperature conditions as described in Table 1.

After assuring that fusion between vesicles occurs and could be monitored with the methods used, in a second study (S2), the fusion between negatively charged (PC/PG/Chol) liposomes and PEGylated liposomes (PC/Chol/PEG) was evaluated in order to better simulate the actual case of fusion between CVs (which are negatively charged) and PEG-liposomes (for final preparation of PEGylated hybrid vesicles).

In all cases, the fusion efficiency was evaluated by FRET dilution [32–34], as described recently [35], after exciting the samples at 460 nm and measuring

**Table 1** Vesicle fusion and hybrid formation protocols

Freeze–thaw cycles [FT] F/T conditions [C] [temp duration]	Sonication (2 min) + incubation (2 h) Incubation temp. (°C)	Sonication (2 min) + incubation (5 h) Incubation temp. (°C)
Study 1 (S1): fusion of neutral liposomes PC/Chol (2:1) with same		
FT-C1: liq N <sub>2</sub> -1 min/40 °C-4 min	37	37
FT-C2: liq N <sub>2</sub> -3 min/37 °C-15 min	45	45
FT-C3: liq N <sub>2</sub> -3 min/50 °C-3 min	60	60
Study 2 (S2): fusion of charged and PEG-liposomes PC/Chol/PEG and PC/PG/Chol		
FT-C2	37	37
FT-C3	45	45
	60	60
Study 3 (S3): fusion of CVs (hCMEC/D3) with PEG liposomes		
FT-C1	-	-
FT-C3	-	-
Study 4 (S4): fusion of CVs (LLC) with PEG liposomes		
FT-C3	-	-

the emission at 530 nm and 588 nm, corresponding to the emissions from NBD and RHO, respectively. The FRET dissolution efficiency of the mixtures was defined as  $E_{FD} = F_{530}/(F_{530} + F_{588})$ , where  $F_{530}$  and  $F_{588}$  represent the fluorescent intensities at 530 and 588 nm, respectively. For calculation of the fusion efficiency a calibration curve was constructed by liposomes containing 0.65, 0.250, and 0.063 mol% of NBD and RHO, which correspond to lipid dilution ratios of 0.65, 2, and 5, respectively [35]. The lipid dilution ratio (LDR) of each labelled mixture was then calculated from the calibration curve. Another measure for liposome fusion is the decrement of the FRET dilution efficiency. Values of % decrement of approx. 25% were reported before for fusion between EVs and (neutral non-PEGylated) liposomes [36].

After completion of the two previous studies, the optimal methodology (which realized highest lipid dilution ratios (or % decrement values)) was selected, and liposome/CV hybrids were formed by fusion of CVs with PC/Chol/PEG liposomes labeled with 1 mol% NBD and 1 mol% RHO. For all further *in vitro* and *in vivo* experiments, liposome/CV hybrids were formed by fusion of CVs (1 mg/mL) with equal volume of unlabeled PC/Chol/PEG liposomes (1 mg/mL).

All hybrids were extruded through polycarbonate membranes with pore sizes of 400 nm (initially) and then 200 nm. Phospholipid content, protein content, and Chol content of hybrids were quantified, as described above. In some cases, hybrids were loaded with FITC, as mentioned above.

## Vesicle characterization

### Size distribution and zeta potential measurements

The particle size distribution (mean hydrodynamic diameter and polydispersity index) of all vesicles, dispersed in 10 mM PBS, pH 7.4 (at 0.4 mg/mL lipid), was measured by dynamic light scattering (Malvern Nano-Zs; Malvern Instruments, Malvern, UK) at 25 °C and a 173° angle. The zeta potential of the same dispersions was measured at 25 °C by use of the Doppler electrophoresis technique.

### TEM

Vesicles (0.5–1 mg/mL) were re-suspended in 10 mM HEPES (to eliminate potential artifacts from phosphate salts) and then negatively stained with 1% phosphotungstic acid in dH<sub>2</sub>O (freshly prepared), washed 3 times with dH<sub>2</sub>O, drained with the tip of a tissue paper, and observed at 100,000 eV with JEM-2100 (Jeol, Tokyo, Japan) transmission electron microscopy (TEM) [37].

## Integrity of vesicles (in vitro)

The integrity of FITC-loaded vesicles was studied by measuring the release of FITC from the vesicles (CVs, hybrids, e-CVs (in which Chol and/or PEG was added) and PEG-LIP (PC/PG/Chol/PEG) which were used for comparison), during incubation in the absence or presence of serum proteins (50% fetal bovine serum v/v (FBS)) for 72 h at 37 °C. FBS was used in addition to PBS in order to understand how stable the various vesicles will be after *in vivo* injection, when they will come in contact with serum proteins [22, 25]. For this, 1 mL of sample (0.5 mL of FITC-loaded vesicles at a lipid concentration of 1 mg/mL mixed with 0.5 mL of media (PBS or FBS)) was added in dialysis tubing sacs (Servapor, with MW cutoff 14,000 Da). The sacs were immersed in 15 mL of PBS buffer in capped test tubes, which were placed in a shaking incubator (Stuart Orbital Incubator) adjusted at 60 rpm, 37 °C. At specified time points (0, 1, 3, 5, 7, 24, 48, 72 h), 2 mL samples were taken from the buffer (volume was replaced with PBS) and FITC was quantified by measuring the sample FI (EX-490 nm/EM-520 nm) by a Shimadzu RF-Fluorescence Spectrophotometer. Sink conditions applied throughout the study.

## Cell studies

### Biocompatibility assay

Biocompatibility of hybrids towards homologous hCMEC/D3 cells was evaluated with the MTT assay. Briefly, 5000 cells were seeded in 96-well plates, and after overnight incubation, medium was replaced with the samples (lipid concentration was 40 µg/mL), and incubated at 37 °C and in 5% CO<sub>2</sub> for 4 h (the maximum incubation period applied in vesicle/cell interaction experiments) or for 48 h. After completion of the cell/vesicle incubations, MTT solution was added in all samples, and after 4 h, acidified isopropanol was used to dissolve the formazan crystals that were formed. Viable cells (%) were calculated based on the equation:  $(A570 \text{ sample} - A570 \text{ background}) / (A570 \text{ control} - A570 \text{ background}) \times 100$ , where A570 control is the OD-570 nm of untreated cells, and A570 background is the OD-570 nm of MTT without cells.

### Cell-uptake studies

For evaluation of the uptake of the various types of vesicles by hCMEC/D3 cells, FITC-loaded vesicles were incubated with confluent cell monolayers (200 nmol lipid/10<sup>6</sup> cells) in RPMI medium, for 4 h at 37 °C. PEG-LIP (PC/PG/



Chol/PEG liposomes) were also studied under identical conditions for comparison. After incubation, the cells were then washed 2 times with ice-cold PBS, detached from plates by scraping, re-suspended in 1 mL of PBS, and assayed for FI (EX-490 nm/EM-520 nm, 5-nm slits) after cell lysis in 2% Triton X-100. Cell auto-fluorescence was always subtracted. Sample protein content was measured by Bradford assay, and FITC uptake was normalized to the protein concentration of each sample. In some cases, the uptake studies were evaluated in hCMEC/D3 cells grown in EndoGro medium.

### Confocal fluorescence microscopy

hCMEC/D3 cells were grown on collagen-covered coverslips and incubated with FITC-labeled vesicles for 4 h. Cells were then fixed in 4% paraformaldehyde for 10 min, stained with Hoechst 33342 for 5 min, and mounted on microscopy slides with Mowiol. Slides were observed using fluorescence microscopy on a SP5 confocal microscope (Leica, Heidelberg, Germany) to visualize their internalization and subcellular distribution. To quantify the cellular uptake of vesicles, all settings of imaging and processing were kept constant and the relative fluorescence intensities were calculated with ImageJ according to the methodology contributed by Luke Hammond (QBI, University of Queensland, Australia) in the open lab book: <https://theolb.readthedocs.io/en/latest/imaging/measuring-cell-fluorescence-using-imagej.html>.

### Mechanism of vesicle uptake by cells

In order to determine whether vesicle uptake is an active or passive process, uptake was additionally estimated after pre-incubation of the cells for 30 min at 4 °C and subsequently incubating the cells for 2 h at 4 °C with FITC-loaded vesicles; the same procedure was also carried out at 37 °C.

To study the potential cellular uptake pathway of each vesicle type, hCMEC/D3 cells were pre-incubated with inhibitors of clathrin and caveolin pathways. For this, before vesicle addition, 10 µg/mL chlorpromazine, or 5 µg/mL filipin were applied to pretreat the cells for 30 min at 37 °C, before incubation of the cells with the vesicles. FITC-loaded vesicles were then added to cells and incubated for 2 h at 37 °C. Cell uptake was calculated as described above.

Confocal microscopy was additionally performed under identical conditions, to verify the effect of inhibitors, by morphological means. In order to exclude the possibility that the inhibitors may induce cellular toxicity under the conditions applying in the uptake experiments, MTT studies were initially carried out. No cytotoxicity was detected.

### In vivo biofluorescence imaging and ex vivo studies

In vivo live animal imaging experiments were performed to estimate the pharmacokinetics and ex vivo organ distribution of hybrids. DiR-labeled vesicles were used because free DiR is rapidly eliminated from mice after injection, as previously verified [25, 38].

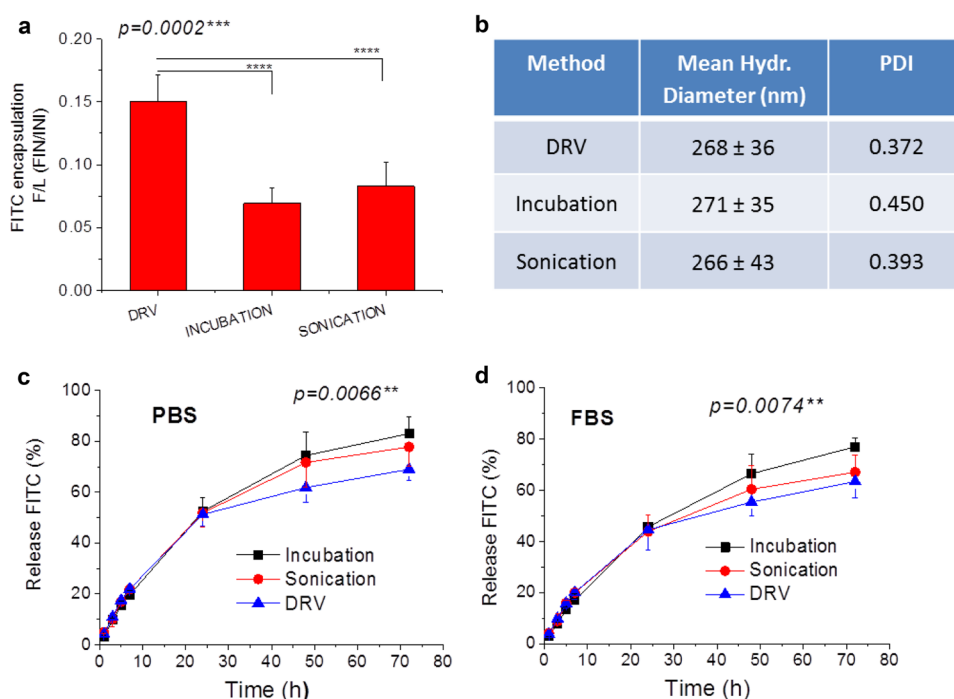
FVB (Friend leukemia virus B) albino mice purchased from Hellenic Pasteur Institute (Athens, Greece), were bred at the Center for Animal Models of Disease, University of Patras, Faculty of Medicine (Rio, Greece). FVB mice were chosen for their white skin and fur that permits enhanced light penetration. Animal care and experimental procedures were approved by the Veterinary Administration Bureau of the Prefecture of Achaia, Greece (protocol approval numbers 3741/16.11.2010, 60291/3035/19.03.2012, and 118018/578/30.04.2014) and were conducted according to Directive 2010/63/EU (European Union 2010) and European Union Directive 86/609/EEC for animal experiments.

The mice were matched for sex (male–female), weight (20–25 g), and age (6–12 weeks). Biofluorescence imaging of living mice and explanted organs was done on an IVIS Lumina II imager (Perkin Elmer, Santa Clara, CA). The mice were anesthetized using isoflurane and were serially imaged at various time points (up to 4 h postinjection, in order to be able to directly compare the current results with previous ones [22]) after retro-orbital injection of DiR-labeled hybrids, CVs and PEG-LIP (200 µg lipid/mouse), as described previously [22, 25, 38]. Retro-orbital venous sinus injection, which is equally effective as tail-vein injection, was used, for avoidance of animal distress and/or retention of significant amounts of the dose in the tail. Standard excitation/emission wavelengths for DiR were applied as follows: excitation 710–760 nm; emission 810–875 nm. The images were acquired and analyzed using Living Image v4.2 software (Perkin Elmer). In detail, specific bodily area or explanted organ regions of interest were created and were superimposed over all images acquired in a uniform fashion, and the photon flux within these regions were measured.

### Statistical analysis

All results are expressed as mean ± SD from at least four independent experiments. Most data were analyzed by using one-way ANOVA followed by Bonferroni post hoc test.  $P < 0.05$  was considered statistically significant for all comparisons. When more factors were compared, two-way ANOVA was performed. The significance of comparisons is presented in the graphs. \* $p < 0.05$ , \*\* $p < 0.01$ , \*\*\* $p < 0.001$ , \*\*\*\* $p < 0.0001$ .

**Fig. 1** **a** Loading of FITC (expressed as FITC/lipid ratio) in CVs from B16 cells, after using different loading methods. **b** Physicochemical properties of the CVs. **c, d** Timeframe of FITC release (% of total) from the various CV types during incubation for up to 72 h (at 37 °C), in PBS and FBS, respectively (significant differences from the control, in each case, are marked with asterisks)



## Results and discussion

### CV engineering methods

#### Engineering methods for drug loading in CVs

As seen in Fig. 1a, B16 cell CVs encapsulated 1.8 and 2.3 times higher amount of FITC when the loading was done using the DRV method, compared to sonication and incubation, respectively; sonication resulted in encapsulation values which were marginally higher than those conferred by incubation. All CV types had similar size distribution (Fig. 1b). Concerning CV integrity, the method used for CV loading (with FITC) was demonstrated to have a significant effect on the release profile of FITC from the vesicles during their incubation in PBS buffer ( $p < 0.01$ ) as well as in FBS ( $p < 0.01$ ), as seen in Figs. 1c, d, respectively). The DRV-loaded vesicles released FITC slightly slower, compared to the vesicles loaded by other methods. The current results confirmed our previous report in which the release of calcein was studied, verifying the superiority of the DRV method as the best method for loading cell-derived vesicles [22]. Compared to the release of calcein from similar CVs prepared by the same methods with the current ones [22], FITC is released slower from all the vesicle types, which is logical due to the larger molecular size of FITC compared to calcein. Additionally, in agreement with previous results about the release of

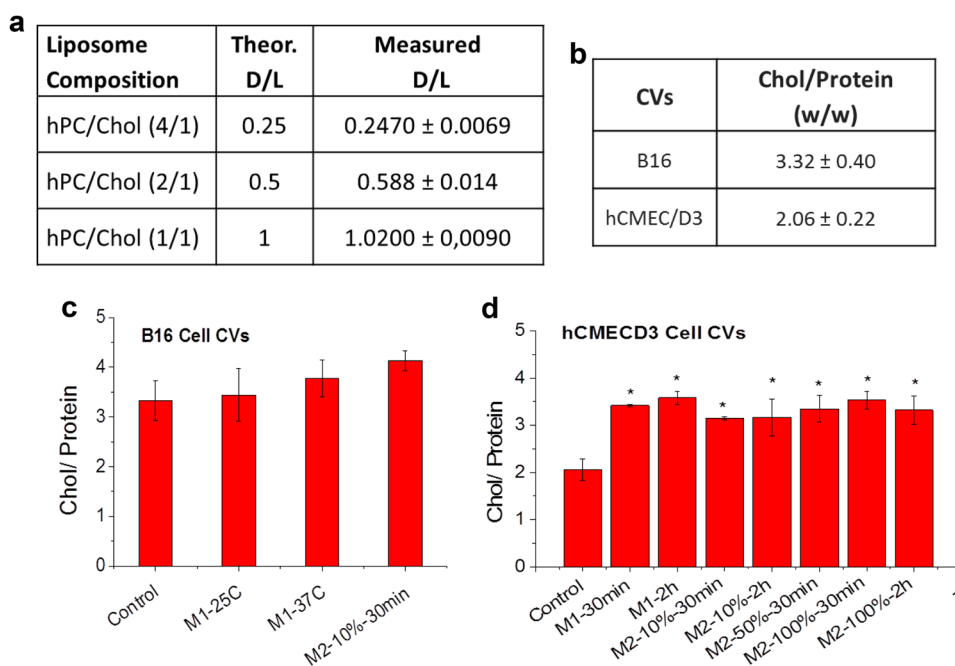
calcein from CVs [22], the release of FITC from CVs (irrespective of the method used for FITC loading) is faster in protein-free buffer compared to FBS, proving that the latter observation was not specific for calcein. In fact the latter phenomenon was previously found to be persistent in three different types of CVs (derived from HEK (hyman embryonic Kidney cells), B16 and hCMEC/D3 cells); thereby, it is additionally not specific for CVs derived from B16 cells.

#### Engineering methods for addition of Chol into CV membranes

As seen in Fig. 2a, the CO/PAP enzymatic method is accurate for the measurement of Chol in lipid membranes, such as liposomes, since the theoretical and measured values are in good agreement. Interestingly, the Chol level of CVs derived from B16 cells is 56% higher than that of CVs from hCMEC/D3 cells (Fig. 2b), explaining why it was not possible to further increase the Chol concentration of the particular CVs, by all the methods applied (Fig. 2c). Oppositely, regardless of the method applied, the Chol content of hCMEC/D3-CVs was always significantly ( $p < 0.05$ ) increased (Fig. 2d).

The significantly lower Chol content of CVs produced from hCMEC/D3 cells compared to CVs produced from B16 cells, which was measured herein (Fig. 2b), may explain the lower integrity of the first CVs compared to the second ones, which was demonstrated before [22]. It is

**Fig. 2** **a** Results of test analyses for verification of the accurate measurement of Chol in liposomes, using the CO/PAP enzymatic method. **b** Cholesterol levels (expresses as Chol/Protein ratio) of CVs derived from B16 and hCMEC/D3 cells. **c, d** Chol content of control and engineered CVs, from B16 cells and hCMEC/D3 cells, respectively, after application of various methods for Chol enrichment (significant differences from the control, in each case, are marked with asterisks)



known that by increasing the Chol content of liposomes, they become more stable, retaining encapsulated hydrophilic molecules for longer time periods; however, the effect of the Chol content of CVs on their stability was never studied before for any type of cell-derived vesicles. From the current results, it is demonstrated that the maximum Chol content of CVs cannot exceed values that confer a Chol/protein level of approx.  $3.5 \pm 0.5$  w/w, even after Chol enrichment is attempted (Fig. 2). Indeed, we also measured the Chol content of HEK cell CVs and found it within the above range ( $3.38 \pm 0.35$ , non-published result), although we did not attempt further Chol enrichment of those CVs. In any case, this finding is interesting and needs to be verified by measuring the Chol/protein content of other CV-types (derived from different parent cells). Furthermore, the effect of adding additional Chol in CVs on their integrity is discussed below.

#### Optimization of method for the coating CVs with PEG

As seen in Fig. 3a, the optimal protocol to coat CVs with PEG is to co-incubate CVs with PEG-micelles at 60 °C for 1 or 2 h. By using different PEG concentrations and applying the above mentioned protocol, it was found that the best PEG concentration to use (the one that realizes the highest decrease of the zeta potential value of the vesicles, which indicates successful coating of the vesicles with PEG) is equal to 10 mol% (of total phospholipid) (Fig. 3b).

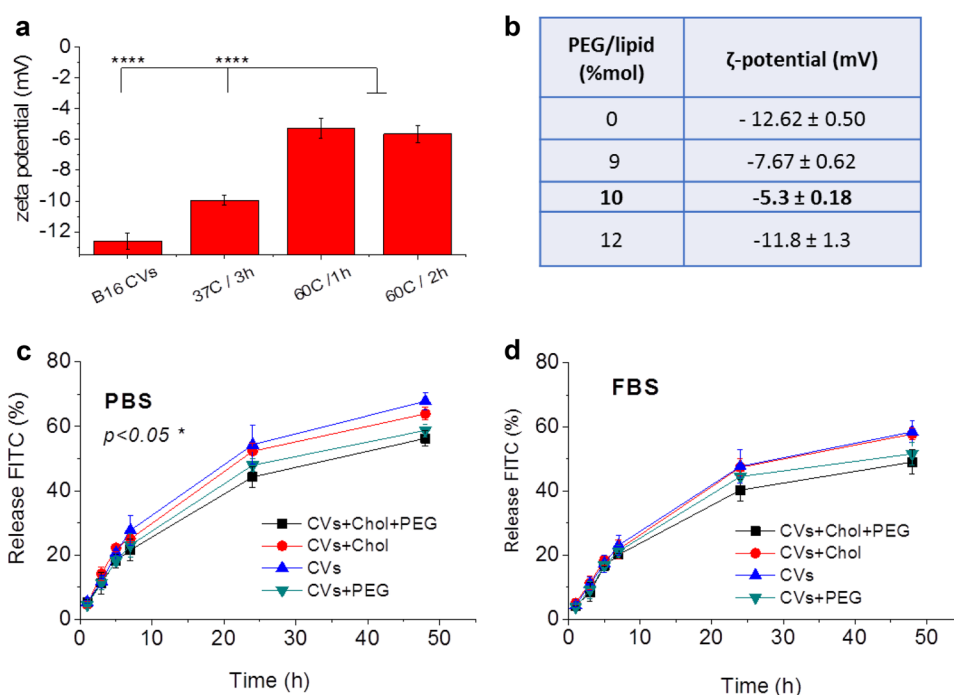
#### Integrity of e-CVs

After identifying the optimal protocols for CV engineering, in order to verify their effects on the integrity of hCMEC/D3 cell-derived CVs, FITC-loaded CVs enriched or not with Chol and/or coated with PEG, were studied for their integrity (release of entrapped FITC) during incubation in PBS and FBS at 37 °C, for 72 h. As seen in Fig. 3c, d, marginal improvements of CV integrity are demonstrated when the vesicles are PEGylated (CVs+PEG), and even more when they are also enriched with Chol (and PEGylated) (CVs+Chol+PEG). However, when the CVs are only enriched with Chol (but not PEGylated), their integrity is not improved, oppositely of what is known for liposomes [39]. When all vesicle types are compared by two-way ANOVA analysis, the vesicle type is seen to significantly ( $p < 0.05$ ) affect the time-frame of FITC release, only when the vesicles are incubated in buffer (Fig. 3c). However, individual comparisons between groups of vesicle types showed that significant differences ( $p < 0.05$ ) for the time-frames of FITC release exist between CVs and CVs+Chol+PEG, and also between CVs+Chol and CVs+Chol+PEG, when incubated in buffer or in FBS.

In accordance with what was mentioned above for the B16-CVs (Fig. 1c, d), all types of hCMEC/D3-CVs also release FITC slower when incubated in FBS, compared to PBS. We do not know why cell-derived vesicles retain their encapsulated materials more during incubation in protein-containing media, compared to plain PBS. The later phenomenon is opposite to what happens in the case



**Fig. 3** **a** Zeta potential values of (PEGylated) e-CVs from B16 cells, produced by applying different protocols for PEGylation. **b** Effect of different PEG concentrations (mol% of total phospholipid) used for CV PEGylation on the zeta potential values of the CVs. **c**, **d** Release (% of total) of FITC from the various CV types (from hCMEC/D3 cells) during incubation for up to 48 h (at 37 °C), in PBS and FBS, respectively (significant differences in each case, are marked with asterisks)



of liposome membranes that are substantially leakier in the presence of serum proteins, due to interactions with serum components (such as lipoproteins) that extract lipid molecules from their membranes leading to leakage of liposome-encapsulated molecules [39]. Perhaps such interactions between serum proteins and CVs are minimized due to the presence of proteins in their membranes.

On the other hand, it is well known that the integrity of liposomes in presence of serum proteins is increased when their Chol content is increased; however, the Chol enrichment of CVs did not have any effect on their integrity, in buffer as well as in FBS. This is particularly strange, when we consider that the Chol/lipid ratios of CVs and Chol-enriched CVs is very high, as seen in Table S1 (Supplementary data). In fact, the Chol/lipid ratios of some CV types (such a B16 CVs and HEK CVs) as well as Chol-enriched CV types (such as Chol-enriched hCMEC/D3 CVs) are practically equal to the maximum amounts that could be incorporated in liposomes since Chol solubility limits of 66 mol% for phosphatidylcholine (PC) bilayers, and 51 mol% for phosphatidyl-ethanolamine (PE) bilayers, have been reported earlier [40]. From all the above mentioned facts, it becomes evident that the protein components of the lipid membrane of CVs and e-CVs are most probably the ones that determine their integrity, as discussed more below.

## Hybrid formation

### Fusion between liposomes

The fusion between liposomes (study 1 and study 2 in Table 1) was initially tested, by applying FT cycle protocols [35] as well as incubation protocols [41], as preliminary studies before the formation of hybrids between CVs and liposomes. The details for all the protocols were evaluated, and all the studies done are seen in Table 1. The physicochemical properties of the various types of liposomes and CVs used for fusion studies are reported in Table 2. The degree of liposomal fusion was evaluated by calculation of LDR values [35] and also % decrement of the FRET dilution efficiency values, as used elsewhere [36].

As seen in Fig. 4, the LDR values after fusion between PC/Chol (2:1) liposomes (study 1, Fig. 4a, b), as well as between PEG-LIP and negatively charged PC/PG/Chol liposomes (study 2, Fig. 4c, d), were lower when the incubation method was applied regardless of incubation time or temperature (Fig. 4a, c), compared to the corresponding values calculated when the FT method was used (Fig. 4b, d). In fact, in the case of fusion between charged and PEG-LIP (Fig. 4d), maximum fusion seems to occur after 5 FT cycles (since the LDR values do not increase when more FT cycles are applied). The same conclusion (judging from the LDR values) can be drawn for the fusion between uncharged liposomes (Fig. 4b), with the exception of protocol FT-C2 for which LDR values increase continuously between 0 and 15 FT cycles.

The same conclusion about the comparison between incubation and FT methods (as above) is drawn by comparing the corresponding % decrement of FRET dilution efficiency values (Fig. 4e for incubation method and Fig. 4f for FT method). Indeed, decrements of about 10% are reported for the incubation protocols, compared to ~ 24% decrements in the case of FT methods, confirming that higher degree of vesicle fusion occurs when FT method is applied. The % decrement values reported herein are close to the values reported before, when hybrids were formed by hydration of thin lipid films with EV dispersions and subjection of the resulting mixtures to vortex and probe sonication or extrusion [36].

In a previous study, the co-presence of PEG (as free molecules) was found to increase the fusion between liposomes and exosomes, during co-incubation of the two types of vesicles at 40 °C for 2 h [41]. In fact, the effect was higher when PEG with increasing MW (up to 8000) was used, and also when increasing amounts of PEG-8000 were used (between 0 and 30% w/v). However, in the same article, it was reported that in absence of PEG, the fusion between liposomes and exosomes after 2 h of co-incubation at 40 °C, was minimum, in agreement with the current results.

### Fusion between CVs and liposomes

After establishing that optimal vesicle fusion occurs by applying the vesicle dispersions to numerous FT cycles, we decided to continue with this methodology for production of hybrid CV-liposome vesicles.

As seen in Fig. 5, where the results of the two studies in which hybrid formation between CVs and liposomes are reported (study 3, for hCMEC/D3-CVs, and study 4, for LLC-CVs), the protocol FT-C3 (cycles of 3 min freezing in liquid Ns followed by 3 min thawing at 50 °C) confers sufficient fusion between the two types of vesicle, as concluded by the significant increase in LDR values (Fig. 5a, b), as well as from the % decrement of the FRET dilution efficiency (Fig. 5c, d). In the case of hCMEC/D3 CVs, we additionally tested the protocol FT-C1 which was not successful to induce CV/liposome fusion (Fig. 5a, c), verifying the decision to continue with protocol FT-C3. In Fig. 5, it is additionally observed that fusion between PEG-LIP and CVs occurs after only 5 FT cycles in the case of

LLC-CVs, while in the case of hCMEC-D3-CVs, a minimum of 15 FT cycles were required for fusion, indicating that perhaps the fusion between liposomes and CVs from LLC cells is easier (compared to CVs from hCMEC/D3 cells). Nevertheless, since we did not measure LDR values between 5 and 15 FT cycles in the specific case, we cannot excluded the possibility that fusion between liposomes and hCMEC/D3-CVs may be completed with less than 15 FT cycles.

The physicochemical properties of the vesicle mixtures were also continuously monitored during vesicle fusion. By comparing the initial physicochemical properties of the vesicle mixtures (mean diameter and PDI) with the values measured after the different fusion protocols were applied (Fig. S1, Supplementary Data), it is seen that the FT method induced significant initial increases in both, the mean vesicle sizes and the PDI-values of the vesicles in study 1 (S1) (Fig. S1A and Fig. S1B, Supplementary Data) and S2 (Fig. S1E and Fig. S1F, Supplementary Data), which after the initial increases gradually decrease, since, most probably any formed fused vesicles (which are probably larger than the initial vesicles) break into smaller vesicles when more FT cycles are applied. Oppositely, the mean diameter and PDI values of the vesicle mixtures were not significantly modified, when the incubation method was applied (Fig. S1C and Fig. S1D for Study 1, as well as Fig. S1G and Fig. S1H for Study 2, Supplementary Data), implying that the vesicles did not fuse (at least to a percent that would cause significant increases of the vesicle size). The later observations are in good agreement with the LDR values reported in the corresponding cases (Fig. 4).

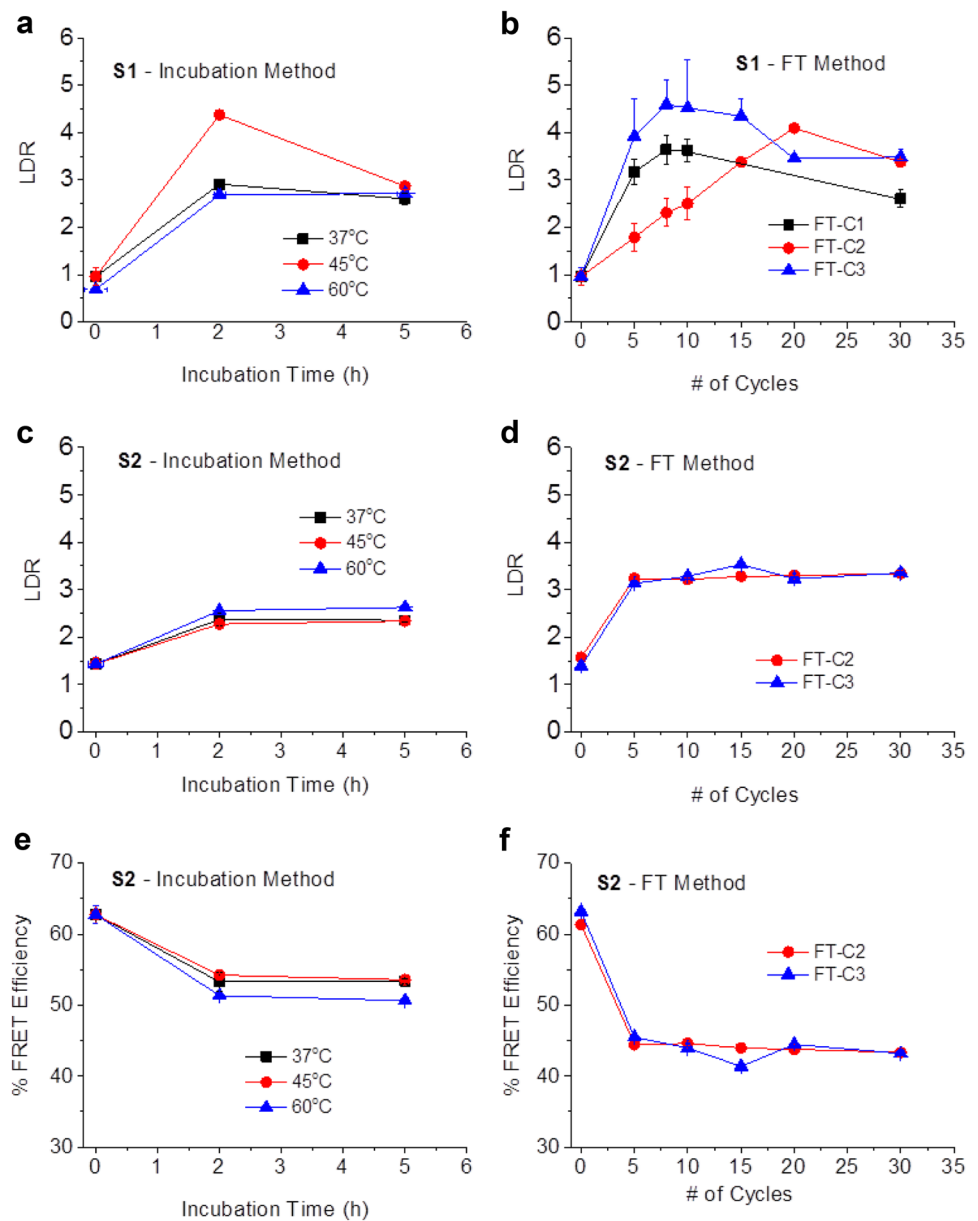
In the case of hCMEC/D3-CV and liposome fusion (as seen in Fig. S1J, Supplementary Data), the FT-C3 protocol confers a significant increase of vesicle size after 5 FT cycles, and after that, the vesicle size progressively decreased as more FT cycles are applied (as observed also in the two cases of fusion between liposomes, S1 and S2, in Fig. 4). On the other hand, the PDI values continuously decreased when more FT-cycles were applied (Fig. S1K, Supplementary Data), which is logical since the initial PDI value of the liposome and CVs mixture is very high, due to the different sizes of the two vesicle populations.

From all the points mentioned above, we can conclude that by monitoring the vesicle size modifications during vesicle fusion, we can obtain valid indications about the

**Table 2** Physicochemical properties of the vesicles used in the hybrid formation studies

Vesicle type	Mean diameter (nm)	PDI	Zeta potential (mV)
PC/Chol LIP	90.2 ± 8.7	0.141 ± 0.052	- 0.487 ± 0.053
PC/Chol/PEG LIP (PEG-LIP)	107 ± 1.1	0.221 ± 0.097	- 3.08 ± 0.68
PC/PG/Chol/PEG LIP (PEG-LIP)	86 ± 1.5	0.212 ± 0.084	- 9.38 ± 0.72
LLC-CVs	269 ± 2.4	0.388 ± 0.087	- 14.4 ± 2.7
hCMEC/D3-CVs	228 ± 3.0	0.450 ± 0.041	- 11.8 ± 2.3

**Fig. 4** Lipid dilution ratio (LDR) values (a–d) and % FRET (dilution) efficiency values (e, f) obtained after fusion of PC/Chol liposomes between them (a, b) and fusion between PEG and negatively charged liposomes (c–f), by applying varying methods and conditions to induce vesicle fusion. Details about the studies (S) and methods are described in Table 1, and in the “Materials and methods” section



extent of vesicle fusion. Both set of results confirm that in all cases of hybrid vesicle formation, 5–15 FT cycles are sufficient for fusion of the vesicles. Furthermore, it is proven that freezing in liquid  $N_2$  for 1 min is not adequate for complete vesicle fusion to occur, while 3 min are. Concluding, the fastest and most efficient protocol for fusion between liposomes and CVs is FT-C3, which involves freezing in liquid  $N_2$  for 3 min and thawing at 50 °C for another 3 min. Depending on the vesicle types involved, between 5 and 15 FT cycles seem to be required. Nevertheless, the possibility that the specific manipulations may jeopardize or decrease the capability of CVs to interact with their target cell types (or in other words decrease their organotropism) should be also evaluated.

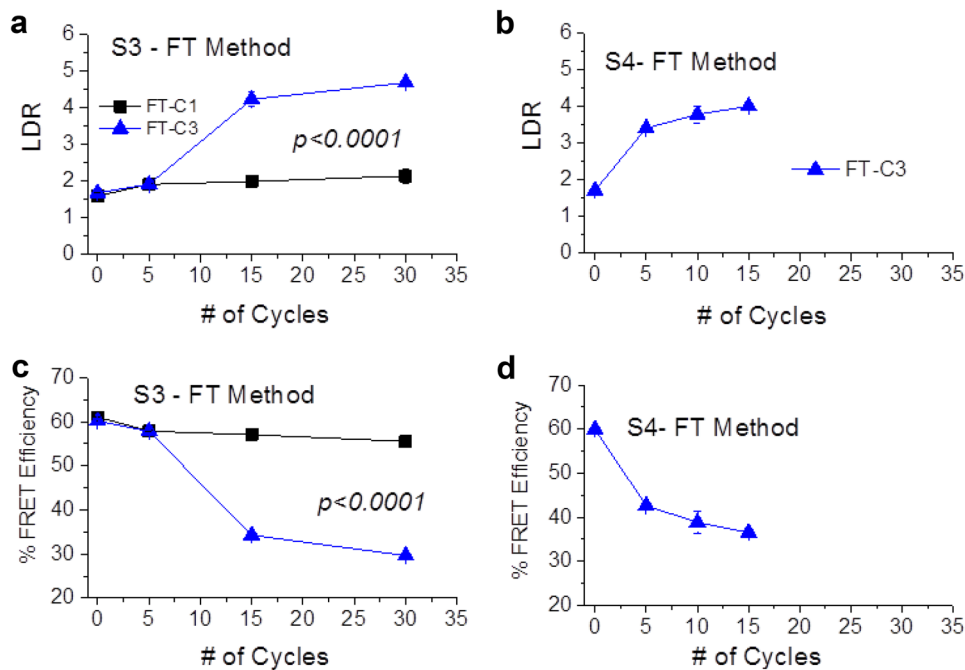
### Comparison of CVs, e-CVs, and hybrids

The various types of cell-derived vesicles were compared for their morphology, their physicochemical properties, and their interaction with hCMEC/D3 cells. Pegylated and negatively charged liposomes (PEG-LIP) were studied under identical conditions, for comparison.

### TEM morphology

As seen in Fig. 6, PEG-LIP, CVs, PEG-LIP, and hybrids have similar round morphology, while their sizes are in agreement to the corresponding size distribution values measured by DLS for each vesicle-type as (see below).

**Fig. 5** LDR (a, b) and %FRET efficiency values (c, d) calculated for the formation of hybrids from PEG-LIP and hCMEC/D3 CVs (a, c), as well as LLC-CVs (b, d), using the FT cycle method



### Vesicle physicochemical properties, integrity, and interaction with cells

Assuming that PEG molecules are completely incorporated in both vesicle types (e-CVs and hybrids), and taking into account that in the case of the e-CVs the PEG molecules are incorporated on the outer layer of the vesicle membrane (so they are exposed on their surface) due to the method used for PEG coating, while in the case of hybrids they are most likely equilibrated between the two layers of the membrane, we calculate that the PEG molecules exposed on the surface of PEG-CVs are approx. 3 times higher than those exposed on the surface of hybrids. In more detail, we calculate that the PEG exposed on the vesicle surface is approximately 10 mol% (of total phospholipids) and 3.12 mol% (of total phospholipids) for e-CVs and hybrids, respectively.

The physicochemical properties of the vesicles used in the vesicle integrity and cell uptake studies are presented in Table 3. As seen, all cell-derived vesicles have similar size distribution values (mean diameter and PDIs), and negative zeta potential; e-CVs have the lowest (absolute) zeta potential (compared to the other two types of cell-derived vesicles) most possibly due to the higher amount of PEG on their surface (in agreement with the calculations mentioned above). The mean diameters of the cell-derived vesicles range between 170 and 214 nm, which agrees with the diameters observed in the TEM micrographs (Fig. 6).

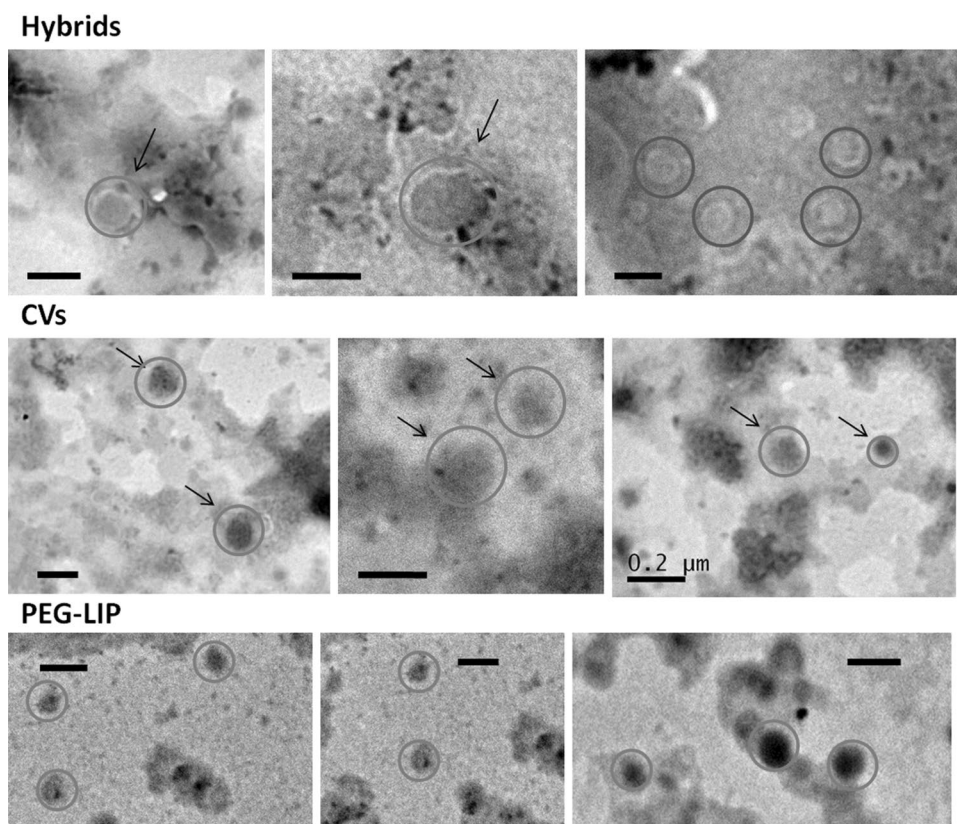
The time-frames of the release of vesicle-encapsulated FITC, during incubation for up to 72 h at 37 °C, when

dispersed in PBS and FBS (50% v/v), are presented in Fig. 7a, b, respectively). As seen, the vesicle type has a significant effect ( $p < 0.0001$ ) on the time-course of FITC release (both in PBS and in FBS), the CVs being the least stable vesicles (compared to all other vesicle types). e-CVs and hybrids seem to have similar integrity, which is higher than that of CVs, but still lower than the integrity of PEG-LIP. Furthermore, it is also seen once more in these results (Fig. 7a, b) that all three types of cell-derived vesicles are more stable when dispersed in FBS compared to PBS, as mentioned also above about the results of Fig. 3. As seen in Fig. 7a, the cell-derived vesicles demonstrate dramatically reduced integrity, compared to PEG-LIP, when dispersed in buffer. The presence of proteins in lipid membranes is known to reduce the stability of membranes, as demonstrated earlier in the case of proteoliposomes [42]. In fact, it was suggested that “the presence of membrane proteins might be responsible for defects in packing at the protein/lipid interphase due to the restricted movement of the phospholipids in the presence of the hydrophobic anchors” [42].

Hybrid vesicles were compared with CVs and PEG-LIP, for their biocompatibility towards hCMEC/D3 cells. As demonstrated by the results of the cytotoxicity study (Fig. S2, Supplementary data), all vesicle types were found to be non-toxic towards hCMEC/D3 cells after co-incubation with the cells for 4 h (the maximum co-incubation period applied when studying vesicle/cell interaction), as well as after 48 h.



**Fig. 6** Representative TEM micrographs of PEG-LIP, CVs (from hCMEC/D3 cells) and hybrids produced by PEG-LIP and CV fusion, using the FT-C3 method (3 min in liq. N2 + 3 min at 50 °C; 30 cycles). The bar in all micrographs corresponds to 200 nm. Circles and arrows are used to denote vesicles



In Fig. 7c, it is observed that the cellular uptake of all types of cell-derived vesicles is substantially higher compared to that of PEG-LIP ( $p < 0.0001$ ). The uptake values follow the order CVs > hybrid s ≥ eCVs > PEG-LIP. The uptake of CVs is slightly higher compared to that of hybrids, but the difference is not significant; however, e-CVs demonstrated significantly lower cell-uptake values ( $p < 0.05$ ) compared to CVs (Fig. 7c). The later result may be explained by the assumption that the PEG coating on the surface of vesicles has a negative effect on their interaction with cells, as reported in several cases before for PEG-LIP [43] and also for PEG-containing EVs [41]. In the same context, the difference in cell-uptake values between hybrids and e-CVs may be based on the different amount of PEG-chains exposed on their surface (Table S1, Supplementary Data).

Concerning the potential mechanisms involved in the uptake of the various types of vesicles, the results of the corresponding experiments are presented in Fig. 7d. First of all, it is observed that for all types of vesicles, vesicle uptake by the cells is energy dependent since the uptake at 37 °C is higher compared to that at 4 °C. As for the effect of the pharmacological inhibitors, it is demonstrated that whereas the uptake of CVs and hybrids is significantly decreased by filipin, but not by chlorpromazine, oppositely the uptake of e-CVs is substantially affected (decreased) by chlorpromazine. Thereby, we may conclude that the uptake of CVs and hybrids

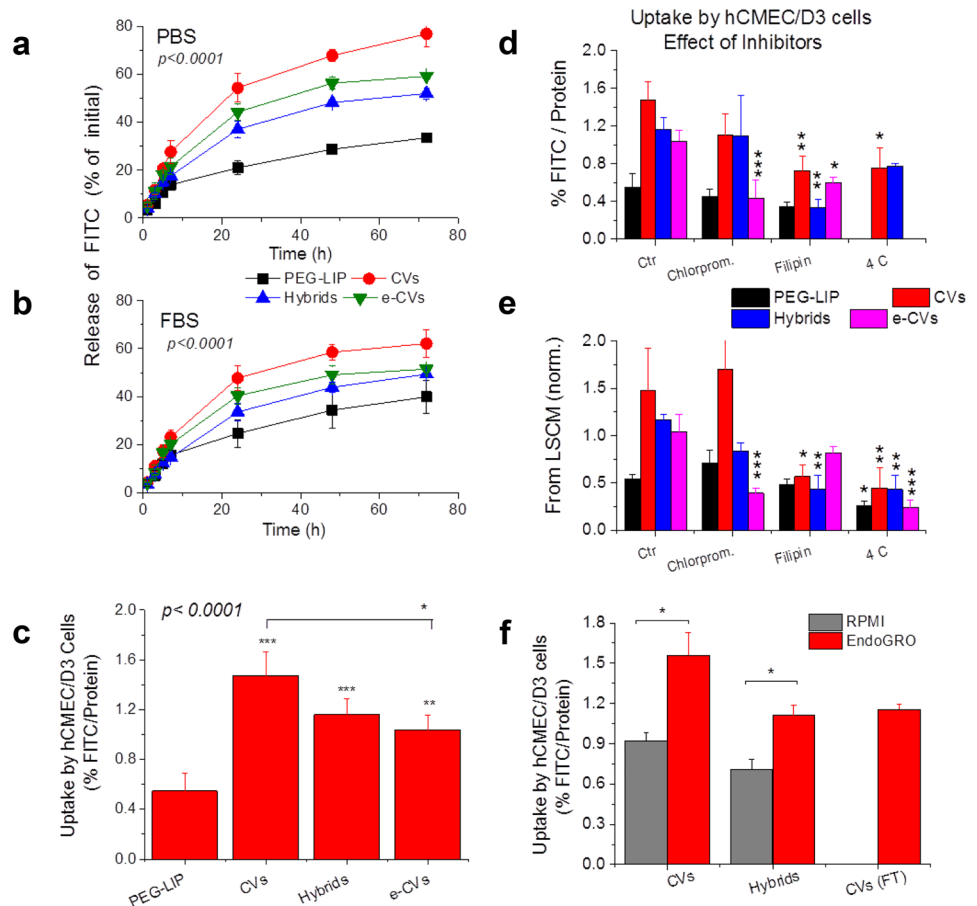
is more dependent on caveolin-related pathways, while e-CVs are mostly taken up by clathrin-dependent pathways. Whether the later difference is related with the higher amount of PEG exposed on the surface of e-CVs (compared to CVs and hybrid vesicles) we cannot be sure. Figure 7 e depicts the results of the same experiments which were carried out by confocal microscopy and subsequent quantification of the fluorescence from the micrographs by ImageJ. In this case, the results for each vesicle type were normalized by setting the initial uptake in absence of inhibitors equal to that measured in the uptake study. As seen, the same conclusions regarding vesicle uptake mechanisms are drawn as those from the results presented in Fig. 7d. In Fig. 8, representative micrographs of the confocal microscopy studies carried out with and without the two inhibitors (filipin (Fil) and chlorpromazine (Chl)), as

**Table 3** Physicochemical properties of the vesicles used in the vesicle integrity studies and the cell uptake studies

Vesicle type	Mean diameter (nm)	PDI	Zeta potential (mV)
PC/PG/Chol/PEG (PEG-LIP)	84.9 ± 9.7	0.191	- 8.5 ± 3.6
CVs	181 ± 39	0.345	- 13.9 ± 1.3
Hybrids	170 ± 25	0.295	- 9.55 ± 0.54
e-CVs	214 ± 23	0.322	- 8.81 ± 0.67



**Fig. 7** (A and B) Timeframe of the release (% of initial) of vesicle-entrapped FITC from the various types of vesicles during incubation in PBS (a) and FCS (b), at 37 °C for up to 72 h. (C) Uptake of the various vesicle types by hCMEC/D3 cells, after 4 h co-incubation at 37 °C. (D) Effect of various cell uptake pathway inhibitors on the uptake of FITC-loaded vesicles by hCMEC/D3 cells after 2 h co-incubation at 37 °C. (E) Similar results as in E, obtained by ImageJ assisted quantification of the LSCM micrographs (representative micrographs are shown in Fig. 7). (F) Uptake of CVs and hybrids, produced by hCMEC/D3 cells grown in RPMI or Endogro medium, by hCMEC/D3 cells, after 4 h co-incubation at 37 °C. Endogro-grown cell-derived CVs were also used after they were subjected to 15 cycles of freeze-thawing (FT) [CVs(FT)]



well as the quantitative total fluorescence intensity values of the microscopy images, are seen.

Finally, in Fig. 7f, the effect of the culturing conditions of the parent cells used for production of cell-derived vesicles (CVs and hybrids), on their cellular uptake, is shown. Both CVs and hybrids produced from hCMEC/D3 cells grown in EndoGro medium demonstrate significantly higher cellular uptake ( $p < 0.05$ ) compared to the same vesicles produced by cells grown in RPMI. The same effect was observed before in the case of CVs [22], and the current results verify the previous ones. Furthermore, the current results reveal that the interaction between hCMEC/D3 cells and hybrids is also influenced by the origin of the CVs which are used for the formation of hybrids, but at a lower extent, which is logical since hybrids have less proteins in the membranes (due to the fact that they are composed by 50% of PEG-LIP that do not contain any proteins in their membranes), compared to CVs. Another very interesting finding is that the uptake of CVs from hCMEC/D3 cells is slightly decreased after the CVs are subjected to FT cycles (Fig. 7f). Although the previous decrease (of % uptake) is not significant (compared to the uptake of CVs), this

may be considered as a drawback for hybrids produced by the FT cycle method.

### In vivo/ex vivo biodistribution

CVs and hybrids from hCMEC/D3 cells were compared also for their in vivo distribution. A live animal imaging experiment was performed using DiR-labeled vesicles, as reported before [22, 25, 38]. The in vivo DiR signals in body and head of animals were measured at predetermined time points, for a period of up to 4 h postinjection. As seen in Fig. 9a, the DiR signals (normalized for DiR dose) of the body (upper graph) and the head (lower graph) of the animals that received PEG-LIP were significantly higher ( $p < 0.001$ ) than those measured in animals injected with CVs or with hybrids; DiR levels measured after hybrid administration (both in heads and bodies) were slightly higher than those measured after CV administration. The lower amounts of DiR in the bodies and heads of animals injected with CVs (compared to PEG-LIP) are easily explained by the fact that there is no PEG on the CV surface and therefore they are rapidly taken up by the RES, as also demonstrated before for CVs derived from hCMEC/D3 cells cultured in EndoGro medium [22]. In the case of the

hybrid vesicles, the similar kinetics with the ones demonstrated for CVs suggest that most probably the PEG content on the surface of the hybrid vesicles may not be sufficient to prolong their circulation in blood, and reduce rapid uptake by the liver and spleen. The latter conclusion is additionally verified by the ex vivo DiR signal data (Fig. 8b). As seen, the animals injected with hybrids, demonstrated significantly higher DiR signals in brain, compared to those injected with CVs; however, similarly increased DiR levels were also measured in the liver and spleen, indicating that although the circulation of hybrids is somewhat improved, compared to that of CVs, this improvement may not be sufficient to significantly enhance their brain targeting potential. In other words, although PEGylated, the hybrids do not seem to be able to avoid their uptake by the RES.

Nevertheless, as seen in Fig. 9, the brain/liver + spleen ratio (B/L+S) (calculated from the corresponding organ DiR signals), which is a measure of the brain-targeting potential of vesicles, is slightly higher for the hybrids, compared to the corresponding value of the CVs, indicating that brain targeting is in fact improved; however, the difference is not statistically significant. On the other hand, the B/L+S ratio calculated for the hybrids is significantly higher than of PEG-LIP.

The current data for in vivo DiR brain signal and ex vivo B/L+S ratio of CVs from hCMEC/D3 cells (grown in RPMI medium) are similar to the ones measured before [22] ( $p = 0.4098$ ), indicating the accuracy and repeatability of the results.

In our previous study, it was reported that CVs from hCMEC/D3 cells which were grown in Endogro medium (in order to express specific membrane proteins that enhance their capability to be transported across the BBB), demonstrated more than two times higher brain targeting potential (B/L+S ratio was equal to  $4.43 \pm 0.77$ ) compared to corresponding CVs from cells grown in RPMI. When the former CVs were engineered (PEGylated and enriched with Chol), their targeting potential was furthermore enhanced by 2.5 times, reaching a B/L+S ratio of  $11.1 \pm 2.1$ . Oppositely, the hybrids developed herein did not demonstrate similar increments regarding their brain targeting potential, compared to the corresponding control CVs.

Nevertheless, it should be noticed that the e-CVs which were studied before [22] had more than two times higher amount of PEG exposed on their surface (compared to the PEG exposed on hybrids surface) which is expected

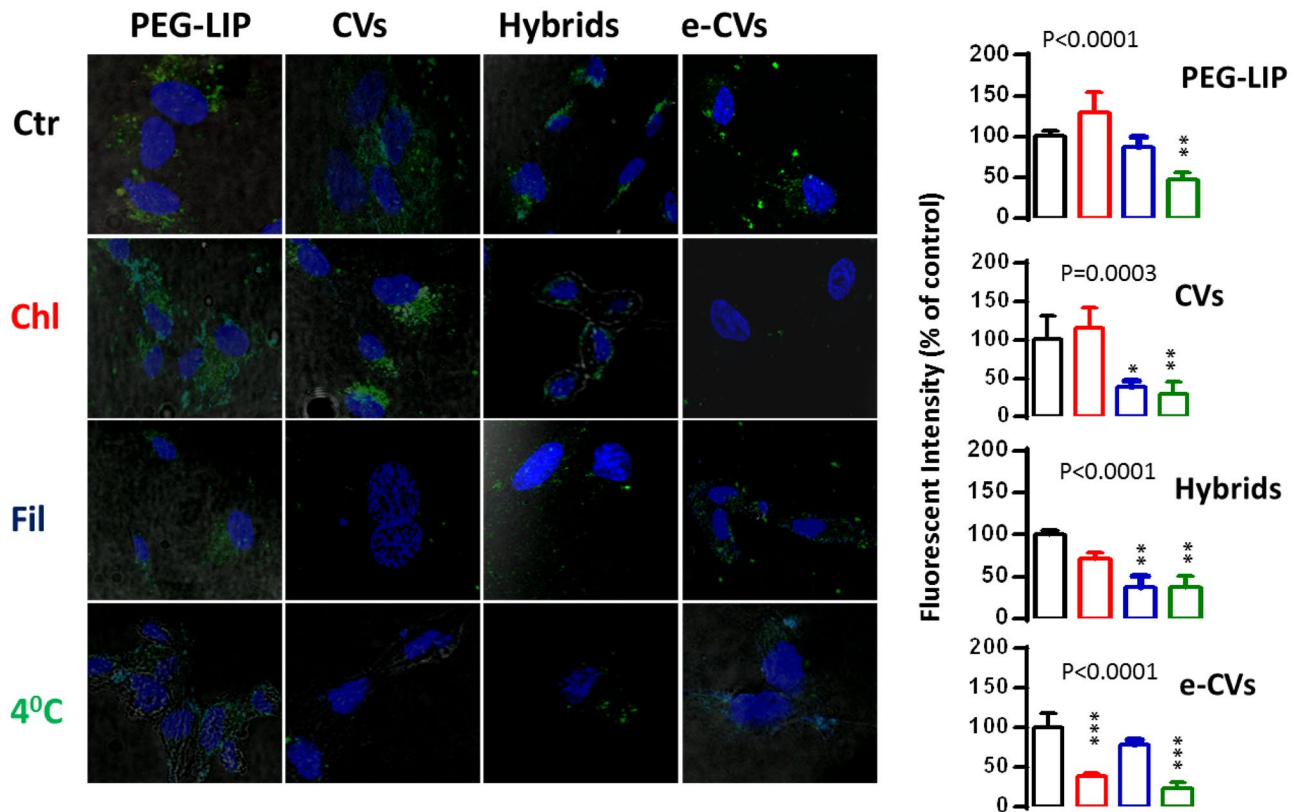


**Fig. 8** Representative micrographs of confocal microscopy studies for the interaction between PEG-LIP, CV, hybrids, and e-CVs, with hCMEC/D3 cells, after 2 h of co-incubation at 37 °C. Ctr micrographs are in absence of inhibitors, while Chl and Fil show the results

following pre-incubation of the cells with chlorpromazine and filipin, respectively. Uptake after co-incubation at 4 °C is also presented. FI values as obtained by ImageJ analysis (normalized to Ct values which were set as 100, for each case), are seen in the right side graphs

to reduce their uptake by the macrophages and their rapid accumulation in the liver and spleen, following iv injection.

## Conclusions

Concerning the methods used for CV loading with therapeutic agents, the current results confirm that the DRV method is significantly more efficient compared to sonication and incubation, verifying our recent report [22] and excluding the possibility that the previous results were specific for calcein (used as a model hydrophilic drug in that case). Furthermore, although the FITC-loaded CVs studied herein, retained higher amounts of encapsulated FITC for longer incubation periods (as anticipated due to the larger MW of FITC) compared to what was reported before for calcein, a slightly improved integrity was still demonstrated for the vesicles loaded by DRV method (compared with those loaded with sonication or incubation) (Fig. 1).

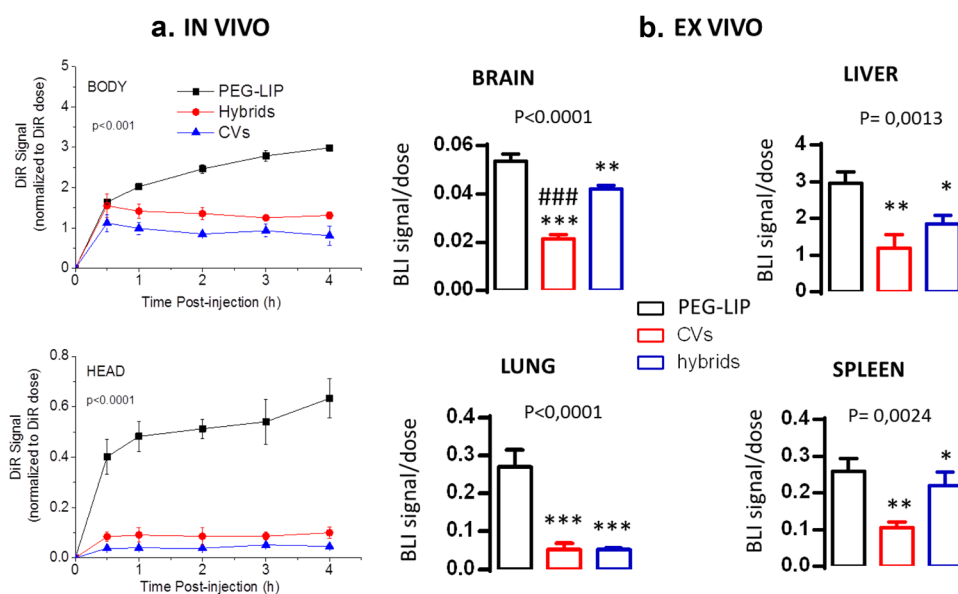
For CV engineering, it was demonstrated that enrichment of vesicle membranes with Chol is possible only when the membranes have a comparably low Chol content; particularly CVs from B16 cells with Chol/protein (w/w)  $\geq 3.3$ , could not be significantly enriched with Chol. For CVs with lower Chol content (such as CVs from hCMED/D3 cells), both types of methods evaluated succeeded to increase their Chol levels (Fig. 2). An optimized method for PEGylation of the surface of CVs was identified; particularly co-incubation of CVs with 10 mol% PEG micelles (compared to total lipid of CVs) at 60 °C was demonstrated to be the most rapid and efficient method.

For hybrid formation, it was proven for the first time that the formation of hybrids between CVs and liposomes is possible, and can be accurately monitored by FRET (Fig. 4

and Fig. 5). Particularly, it was demonstrated that 5 (or 15 in some cases) FT cycles results in complete fusion of CVs with liposomes, while simple incubation at 37–60 °C, even for prolonged duration (up to 5 h) is not as efficient as the FT method. Nevertheless, it should be considered that after CVs were subjected to 15 FT cycles their uptake by hCMED/D3 brain cells was slightly decreased (Fig. 7f).

Considering the integrity of CVs, e-CVs and hybrids, compared to that of liposomes, the previous finding that calcein-loaded CVs are more stable in presence of serum proteins than in buffer [22], was verified with FITC-loaded CVs. Additionally similar behaviors were observed for e-CVs and hybrid vesicles; the latter is probably attributed to the protein content of the membranes produced from cells, it agreement with previous reports about defects in packing at protein/lipid inter-phases [42]. It was additionally found that the integrity of cell-derived vesicles could only be enhanced by coating their surface with PEG (Fig. 3 and Fig. 7); the enrichment of CV membranes with Chol did not produce significantly more stable vesicles (Fig. 3). Furthermore, the higher integrity of e-CVs (based on the "Retention in FBS / Retention in PBS" ratio, as derived from the results of Fig. 7a and Fig. 7b) compared to hybrids is most possibly attributed to the fact that the former vesicles have higher PEG concentration on their surface, compared with the later (Fig. 7). However, although the higher amounts of PEG exposed on the surface of e-CVs enhanced their integrity compared to hybrids, the same is probably the reason for their decreased interaction with cells (Fig. 7 and Fig. 8), as reported before for liposomes and EVs [41, 43]. The current results about the effect of the culturing media of parent cells on the tropism of the CVs (Fig. 7f), confirm and extend our previous findings [22], since the same effect was also demonstrated in the case of the hybrid vesicles that were produced from the CVs. It is

**Fig. 9** **a** In vivo DiR signals (normalized according to the exact total Signal of the dose injected) in the bodies (BODY, upper graph) and heads (HEAD, lower graph), of animals injected with PEG-LIP, CVs (from hCMED/D3 cells) and hybrids, at various time points, up to 4 h postinjection. **b** Ex vivo DiR signals measured in organs 4 h post-injection of PEG-LIP, CVs (from hCMED cells grown in RPMI medium), and hybrids



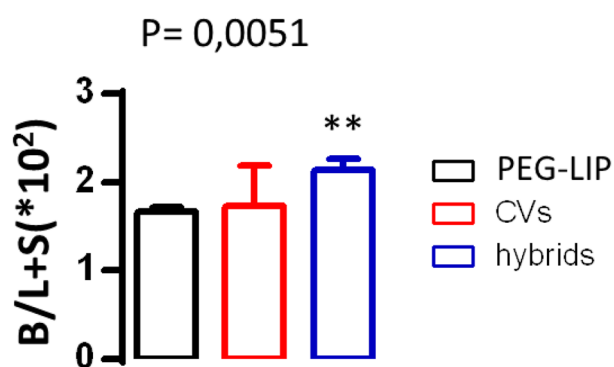


**Fig. 10** Brain/liver + spleen (B/L+S) ratios calculated from the ex vivo DiR signals measured in the brain, liver, and spleen, 4 h postinjection of animals with PEG-LIP, CVs (from hCMEC/D3 cells grown in RPMI medium) and hybrids

known that when hCMEC/D3 cells are cultured in EndoGro medium they express specific proteins on their membranes, which contribute to the formation of “tight” cell monolayers [44]. Furthermore, we recently identified significant differences in the proteome of the two CV types (derived from cells grown in RPMI and EndoGro) by proteomic analysis [22].

The current in vivo and ex vivo results show that despite the slight increase in % DiR in brain compared to the CVs originating from the same type of cells, the particular hybrid vesicles tested herein do not seem to be capable to profoundly increase the brain delivery of encapsulated substances. The later conclusion can be attributed to two possible factors. One factor is the “dilution” of the membrane proteins (which are responsible for the increased brain targeting by CVs from hCMEC/D3 cells) in the hybrids; this suggestion agrees with the slightly lower uptake of the hybrids by hCMEC/D3 cells (Fig. 6), although the later may also be influenced by the presence of PEG on the hybrids (even if it is a low amount). A second factor is attributed to the amount of PEG exposed on the surface of the hybrids, which is probably not enough to provide the required stealth characteristics to the hybrid vesicles, in order to avoid rapid uptake by RES. When the current in vivo and ex vivo biodistribution results for hybrids are compared with those reported for e-CVs [22], the importance of the amount of vesicle surface exposed PEG, becomes evident. The current results prove that it is important to increase the amount of surface exposed PEG on hybrids, by using liposomes with higher PEG concentration (than the current 8 mol%) for their formation, or by adding PEG-micelles in the liposome-CV mixtures, in future studies. In the same context, e-CVs are probably more efficient targeted drug carriers (of cellular origin), compared to hybrids.

**Supplementary Information** The online version contains supplementary material available at <https://doi.org/10.1007/s13346-021-00900-1>.

**Acknowledgments** Authors are thankful to Dr. Mary Kollia and the Laboratory of Electron Microscopy and Microanalysis (L.E.M.M.), Faculty of Natural Sciences, University of Patras, for the TEM studies. The help provided in capturing confocal images by Dr Magda Spella, University of Patras, is highly acknowledged.

**Author contributions** AM and MK: experiment execution, analysis of results; preparation of spreadsheets of results and graphs; participation in writing and in conceptualization. GTS: provided materials and equipment; design of in vivo studies; participation in writing, statistical analysis, and conceptualization; SGA: conceptualization and design of studies, writing of final draft, supervision during experiment execution. PI: funding programs.

**Funding** Financial support was provided to AM by the Stavros Niarchos Foundation within the framework of the project ARCHERS (“Advancing Young Researchers’ Human Capital in Cutting Edge Technologies in the Preservation of Cultural Heritage and the Tackling of Societal Challenges”). M.K., A.M. and S.G.A. acknowledges the support by the project: “Development of Innovative Neuroprotective Neurogenerative Synthetic Micro-Neurotrophins” (MIS-5032840) which is implemented under the Special Service of the Operational Program Competitiveness Entrepreneurship and Innovation. The project is funded by the Operational Programme “Competitiveness, Entrepreneurship and Innovation” (NSRF 2014–2020) and co-financed by Greece and the European Union (European Regional Development Fund).

**Data availability** All raw data are available if needed.

## Compliance with ethical standards

**Conflict of interests** The authors declare that they have no conflict of interest.

**Ethics approval** Animal care and experimental procedures were approved by the Veterinary Administration Bureau of the Prefecture of Achaia, Greece (protocol approval numbers 3741/16.11.2010, 60291/3035/19.03.2012, and 118018/578/30.04.2014) and were conducted according to Directive 2010/63/EU (European Union 2010) and European Union Directive 86/609/EEC for animal experiments.

**Consent to participate** All authors have consented to participate in the studies carried out for this publication.

**Consent for publication** All authors have consented with this publication.

## References

1. Antimisariaris SG, Mourtas S, Marazioti A. Exosomes and exosome-inspired vesicles for targeted drug delivery. *Pharmaceutics*. 2018;10(4):218.
2. Patil SM, Sawant SS, Kunda NK. Exosomes as drug delivery systems: a brief overview and progress update. *Eur J Pharmac Biopharmac*. 2020;154:259–69.
3. Mehryab F, Rabbani S, Shahhosseini S, Baharvand H, Haeri A. Exosomes as a next-generation drug delivery system: An

- update on drug loading approaches, characterization, and clinical application challenges. *Acta Biomater.* 2020;113:42–62.
4. Jang SC, Kim OY, Yoon CM, Choi DS, Roh TY, Park J, Nilsson J, Lötqvall J, Kim YK, Gho YS. Bioinspired exosome-mimetic nanovesicles for targeted delivery of chemotherapeutics to malignant tumors. *ACS Nano.* 2013;7:7698–710.
  5. Zheringer E, Barta T, Li M, Vlassov A. Strategies for isolation of exosomes. *Cold Spring Harb Protoc.* 2015;2015:319–23.
  6. Heinemann ML, Ilmer M, Silva LP, Hawke DH, Recio A, Vorontsova MA, Vykoukal J. Benchtop isolation and characterization of functional exosomes by sequential filtration. *J Chromatogr A.* 2014;1371:125–35.
  7. Jo W, Kim J, Yoon J, Jeong D, Cho S, Jeong H, Yoon YJ, Kim SC, Gho YS, Park J. Large-scale generation of cell-derived nanovesicles *Nanoscale.* 2014;6:12056–64.
  8. Yoon J, Jo W, Jeong D, Kim J, Jeong H, Park J. Generation of nanovesicles with sliced cellular membrane fragments for exogenous material delivery. *Biomaterials.* 2015;59:12–20.
  9. Lunavat TR, Jang SC, Nilsson L, Park HT, Repiska G, Lässer C, Nilsson JA, Gho YS, Lötqvall J. RNAi delivery by exosome-mimetic nanovesicles—Implications for targeting c-Myc in cancer. *Biomaterials.* 2016;102:231–8.
  10. Goh WJ, Lee CK, Zou S, Woon EC, Czarny B, Pastorin G. Doxorubicin-loaded cell-derived nanovesicles: an alternative targeted approach for anti-tumor therapy. *Int J Nanomed.* 2017;12:2759–67.
  11. Goh WJ, Zhou S, Ong WY, Torta F, Alexandra AF, Schiffelers RM, Storm G, Wang JW, Czarny B, Pastorin G. Bioinspired cell-derived nanovesicles versus exosomes as drug delivery systems: a cost-effective alternative. *Sci Rep.* 2017;7:14322.
  12. Wu JY, Ji AL, Wang ZX, Qiang GH, Qu Z, Wu JH, Jiang CP. Exosome-mimetic nanovesicles from hepatocytes promote hepatocyte proliferation in vitro and liver regeneration in vivo. *Sci Rep.* 2018;8:2471.
  13. Villata S, Canta M, Cauda V. Evs and bioengineering: From cellular products to engineered nanomachines. *Inter J Mol Sciences.* 2020;21(17):6048.
  14. Meng Y, Asghari M, Aslan MK, Stavarakis S, deMello AJ. Microfluidics for extracellular vesicle separation and mimetic synthesis: Recent advances and future perspectives. *Chem Engineer J.* 2021;404:126110.
  15. Vázquez Ríos AJ, Molina-Crespo A, Bouzo BL, López-López R, Moreno-Bueno G, de la Fuente M. Exosome mimetic nanoplatfoms for targeted cancer drug delivery *J Nanobiotechnol.* 2019;17:85.
  16. Zha Y, Lin T, Li Y, Zhang S, Wang J. Exosome-mimetics as an engineered gene-activated matrix induces in-situ vascularized osteogenesis. *Biomaterials.* 2020;247:119985.
  17. Lin T, Zha Y, Zhang X, Wang J, Li Z. Gene-activated engineered exosome directs osteoblastic differentiation of progenitor cells and induces vascularized osteogenesis in situ. *Chem Engineer J.* 2020;400:125939.
  18. Hwang DW, Choi H, Jang SC, Yoo MY, Park JY, Choi NE, Oh HJ, Ha S, Lee YS, Jeong JM, Gho YS, Lee DS. Noninvasive imaging of radiolabelled exosome-mimetic nanovesicles using <sup>99m</sup>Tc-HMPAO. *Sci Rep.* 2015;5:15636.
  19. Wiklander OPB, Nordin JZ, O’Loughlin A, Gustafsson Y, Corso G, Mager I, Vader P, Lee Y, Sork H, Seow Y, Heldring N, Alvarez-Erviti L, Smith CIE, Le Blanc K, Macchiarini P, Jungebluth P, Wood MJA, Andaloussi EL, S. Extracellular vesicle in vivo biodistribution is determined by cell source, route of administration and targeting. *J Extracell Vesicles.* 2015;4:26316.
  20. Morishita M, Takahashi Y, Nishikawa M, Takakura Y. Pharmacokinetics of Exosomes: An Important Factor for Elucidating the Biological Roles of Exosomes and for the Development of Exosome-Based Therapeutics. *J Pharm Sciences.* 2017;106:2265–9.
  21. Kooijmans S, Fliervoet L, Van Der Meel R, et al. PEGylated and targeted extracellular vesicles display enhanced cell specificity and circulation time. *J Control Release.* 2016;224:77–85.
  22. Marazioti A, Papadia K, Kannavou M, Spella M, Basta A, de Lastic AL, Rodi M, Mouzaki A, Samiotaki M, Panayotou G, Stathopoulos GT, Antimisariis SG. Cellular vesicles: new insights in engineering methods, interaction with cells and potential for brain targeting. *J Pharmacol Exp Ther.* 2019;370(3):772–85.
  23. Ying M, Zhuang J, Wei X, Zhang X, Zhang X, Jiang Y, Dehaini D, Chen M, Gu S, Gao W, et al. Remote-loaded platelet vesicles for disease-targeted delivery of therapeutics. *Adv Funct Mater.* 2018;28:1801032.
  24. Zhang X, Angsantikul P, Ying M, Zhuang J, Zhang Q, Wei X, Jiang Y, Zhang Y, Dehaini D, Chen M, et al. Remote loading of small-molecule therapeutics into cholesterol-enriched cell-membrane-derived vesicles. *Angew Chem Int Ed Engl.* 2017;56:14075–9.
  25. Markoutsas E, Papadia K, Giannou AD, Spella M, Cagnotto A, Salmons M, Stathopoulos GT, Antimisariis SG. Mono and dually decorated nanoliposomes for brain targeting, in vitro and in vivo studies. *Pharm Res.* 2014;31(5):1275–89.
  26. Antimisariis SG. Preparation of DRV liposomes. *Methods Mol Biol.* 2017;1522:23–47.
  27. Stewart JC. Colorimetric determination of phospholipids with ammonium ferrioxalate. *Anal Biochem.* 1980;104:10–4.
  28. Zidovetzki R, Levitan I. Use of cyclodextrins to manipulate plasma membrane cholesterol content: evidence, misconceptions and control strategies. *Biochim Biophys Acta.* 2007;1768(6):1311–24.
  29. Klein U, Gimple G, Fahrenholz F. Alteration of the myometrial plasma membrane cholesterol with b-cyclodextrin modulates the binding affinity of the oxytocin receptor. *Biochemistry.* 1995;34:13784–93.
  30. Allain CC, Poon LS, Chan CS, Richmond W, Fu PC. Enzymatic determination of total serum cholesterol. *Clin Chem.* 1974;20(4):470–5.
  31. Richmond W. Preparation and properties of a cholesterol oxidase from *Nocardia* sp. and its application to the enzymatic assay of total cholesterol in serum. *Clin Chem.* 1973;19(12):1350–6.
  32. Pick U. Liposomes with a large trapping capacity prepared by freezing and thawing of sonicated phospholipid mixtures. *Arch Biochem Biophys.* 1981;212:186–94.
  33. Oku N, MacDonald RC. Differential effects of alkali metal chlorides on formation of giant liposomes by freezing and thawing and dialysis. *Biochemistry.* 1983;22:855–63.
  34. Macdonald RI, Macdonald RC. Lipid mixing during freezing thawing of liposomal membrane as monitored by fluorescence energy transfer. *Biochim Biophys Acta.* 1983;735:243–51.
  35. Sato YT, Umezaki K, Sawada S, Mukai A, Sasaki Y, Harada N, Shiku H, Akiyoshi K. Engineering hybrid exosomes by membrane fusion with liposomes. *Scientific Reports.* 2016;6:21933.
  36. Rayamajhi S, Nguyen TDT, Marasini R, Aryal S. Macrophage-derived exosome-mimetic hybrid vesicles for tumor targeted drug delivery. *Acta Biomater.* 2019;94:482–94.
  37. Franken LE, Boekema EJ, Stuart MCA. Transmission electron microscopy as a tool for the characterization of soft materials: application and interpretation. *Adv Sci.* 2017;4:1600476.
  38. Papadia K, Giannou AD, Markoutsas E, Bigot C, Vanhoute G, Mourtas S, Van der Linded A, Stathopoulos GT, Antimisariis SG. Multifunctional LUV liposomes decorated for BBB and amyloid targeting - B. In vivo brain targeting potential in wild-type and APP/PS1 mice. *Eur J Pharm Sciences.* 2017;102:180–7.
  39. Antimisariis SG, Kallinteri P, Fatouros DG. Liposomes and drug delivery. In *Pharmaceutical manufacturing handbook* (ed. S Cox Gad) Hoboken, NJ: John Wiley and Sons, Inc. 2007;443–533.



40. Huang J, Buboltz JT, Feigenson GW. Maximum solubility of cholesterol in phosphatidylcholine and phosphatidylethanolamine bilayers. *Biochim Biophys Acta*. 1999;1417:89–100.
41. Piffoux M, Silva AKA, Wilhelm C, Gazeau F, Taresté D. Modification of extracellular vesicles by fusion with liposomes for the design of personalized biogenic drug delivery systems. *ACS Nano*. 2018;12(7):6830–42.
42. Elferink MGL, de Wit JG, Veld GI, Reichert A, Driessen AJM, Ringsdorf H, Konings WN. The stability and functional properties of proteoliposomes mixed with dextran derivatives bearing hydrophobic anchor groups. *Biochim Biophys Acta*. 1992;1106:23–30.
43. Allen TM, Cullis PR. Liposomal drug delivery systems: from concept to clinical applications. *Adv Drug Deliv Rev*. 2013;65:36–48.
44. Schrade A, Sade H, Couraud PO, Romero IA, Weksler BB, Niewoehner J. Expression and localization of claudins-3 and -12 in transformed human brain endothelium. *Fluids Barriers CNS*. 2012;9:6.

**Publisher's Note** Springer Nature remains neutral with regard to jurisdictional claims in published maps and institutional affiliations.